Archaeometry **48**, 3 (2006) 481–499. Printed in Singapore

ANALYTICAL CHARACTERIZATION OF ROMAN PLASTERS OF THE '*DOMUS FARINI*' IN MODENA*

P. BARALDI,[1] A. BONAZZI,[2] N. GIORDANI,[3] F. PACCAGNELLA[1] and P. ZANNINI[1]

[1]*Dipartimento di Chimica, Università di Modena e Reggio Emilia, Via Campi 183, 41100, Modena, Italy*
[2]*Dipartimento di Scienze della Terra, Università di Parma, Parco Area delle Scienze, 157A, 43100, Parma, Italy*
[3]*Soprintendenza ai Beni Archeologici dell'Emilia Romagna, Via delle Belle Arti n. 52, 40100, Bologna, Italy*

The paper refers to the analytical characterization of Roman painted plasters dating back to the second century AD. *The following techniques were used: optical microscopy (OM), scanning electron microscopy (SEM–EDS), micro-Raman and Fourier transform infrared spectroscopies (μ-Raman and FT–IR), X-ray diffraction (XRPD), colorimetry and thermal analyses (TG/DTA).*

The investigation analysed the chemical composition and structure of the plasters, the chemical composition of the pigment layers, the use of binders and any chemical alteration of pigments as well as deterioration of the samples. Stratigraphic analysis of plasters allowed identification of their individual components, which proved helpful in finding out more about the mural painting technique employed.

KEYWORDS: ROMAN PLASTERS, MICRO-RAMAN, FT–IR, SEM–EDS, XRPD, TG/DTA

INTRODUCTION

Research aims

Plasters from *Domus* in northern Italy ascribable to the Roman age are frequently found during both random and programmed excavation (Casoli 1999). While archaeological studies abound, scientific ones remain few and far between, and it is only in recent times that extensive investigations (Baraldi 2001; Fagnano *et al*. 2003; Mazzocchin *et al*. 2004) in other *Regiones* have been carried out. The numerous excavations made in the *VIII Regio*, in the 19th and 20th centuries, generated a collection of plaster fragments—exhibited in the Museums of Parma (Baraldi *et al*. 2005), Reggio Emilia, Modena, Bologna and Forlì—that is extensive but has yet to be studied thoroughly. The first research task, then, was to identify the palette of pigments used by the painters or craftsmen in the *VIII Regio*, especially those of *Mutina* in the first and second centuries AD. Such data allow for comparison with other nearby towns and, more generally, with the palettes of well-known sites from the same epoch, such as Rome and Pompeii. Moreover, these data permit comparison of the different mural painting techniques used in the Roman period, in *Mutina* and in the region of *Emilia Romagna*, with samples discovered in other areas of northern Italy.

There are few original sources on Roman mural painting; the only reference manuscripts are Pliny's *Naturalis historia*, Vitruvius' *De architectura* and Heraclius' *De coloribus et artibus Romanorum*. Therefore, we can only assume that the artists of this period proceeded as

*Received 29 March 2005; accepted 15 August 2005.

described in these manuscripts. In his *Il libro dell'arte* (at the beginning of the 15th century), Cennino Cennini provides an in-depth description of the making of plasters and 'frescoes'. However, the most important text is, perhaps, that of Augusti (1967), which illustrates both concepts and materials and provides sound interpretation of numerous facts regarding the Imperial-age paintings of Pompeii.

The painted plasters of the 'Domus Farini' *in Modena*

Fragments of painted plasters were found during the excavation of a Roman *Domus* in downtown Modena (Via Farini), which would once have been located inside the *castrum* of *Mutina*, north of the *via Aemilia*. The fragments are now preserved in the Archaeological Civic Museum of Modena. Previous historical/art studies have ascribed them to the second century AD (Casoli 1999), in the late Republican age.

A full understanding of the overall structure of this *Domus* decoration is impossible because the plasters are so fragmented. However, it can be supposed that all the samples came from the same room(s), as they have a homogenous pattern of decoration. Archaeologists have been able to reconstruct a section of wall by observing the patterns found on the pieces and studying the stratigraphy of the plasters (Fig. 1).

During the excavation, the remains of a mosaic floor consisting of black and white *tesserae* was documented; fragments of black-varnished pottery and plasters and some utensils were also found.

The samples at our disposal consisted of 37 pieces of wall painting, with approximate dimensions from 2×5 to 8×15 cm.

Since the aim of the analyses illustrated in this paper was to understand as much as possible about the pigment palette and the plaster application/painting techniques, it was important that

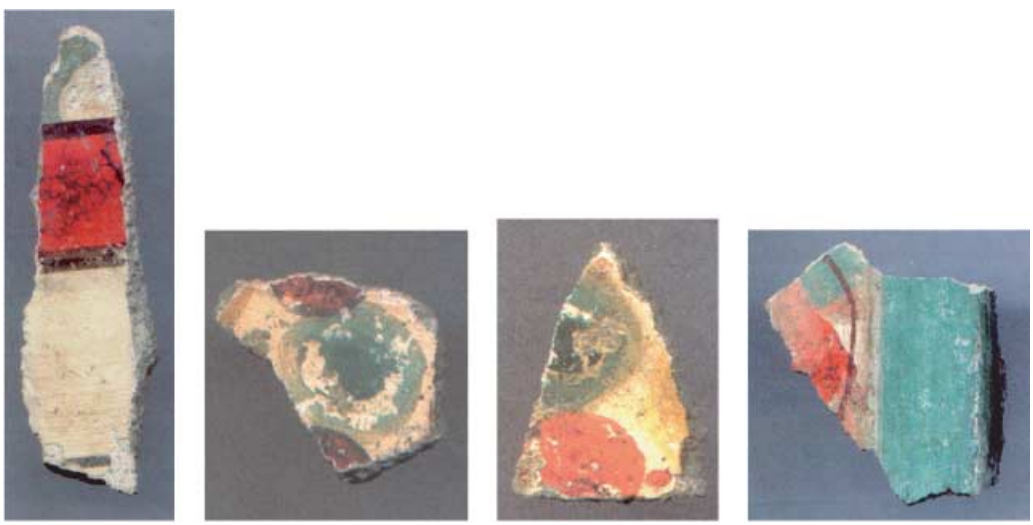

Figure 1 *Four typical fragments and examples of the different typology of the coloured surfaces.*

they should be preserved well. Fortunately, some samples from the '*Domus Farini*' are in a good condition, having brilliant colours and smooth surfaces.

EXPERIMENTAL

The choice of analytical methodology

The analytical techniques utilized in this work were OM, SEM–EDS, μ-Raman and FT–IR spectroscopy, XRPD, colorimetry and thermal analyses.

Because some of these techniques are destructive, the first difficulty was proper sampling, which meant assessing whether the experiment should best be conducted in a destructive, micro-destructive or non-destructive way (Bèarat *et al*. 1997; Ciliberto and Spoto 2000; Colinart and Menu 2001).

As is well known, μ-Raman spectroscopy and colorimetry are not destructive; the other techniques are micro-destructive, so they were used to analyse only very small samples (a few milligrams). Where possible, the required quantity was taken from the tiny pieces that spontaneously detach from mural paintings following deterioration; this meant that samples could be obtained without damaging the surface of the artefact.

To make stratigraphic analysis easier, the 37 samples were prepared as cross-sections. Samples were enveloped in epoxy resin, polished and photographed with an optical microscope at 100× magnification (to give an initial idea of the stratigraphy) to provide a reference for subsequent analyses.

SEM–EDS

Morphological imaging and further analyses were carried using a scanning electron microscope (Philips XL 40, with EDS, Oxford INCA system) with an acceleration potential of 20–25 keV and an average counting time of 100 live seconds.

All the surfaces and fragmented powders were analysed by SEM, attaching them to aluminium stabs with an Ag-conductive glue and enhancing conductivity by coating surfaces with approximately 5 nm of metallic gold.

Micro-Raman spectroscopy

Micro-Raman analysis of the surfaces of the fragments was made by placing them under the microscope with the painted surface to be identified facing upwards and perpendicular to the laser.

So as to identify a homogeneous target for punctual analysis, numerous spectra were collected for each section; reference was also made to the cross-section photographs taken with the optical microscope.

The Raman spectra were obtained using a confocal Jobin Yvon Labram Raman microscope, employing the 632.8 nm line and a power of about 1 mW. The detector was a 1100-pixel CCD (330 × 1100) cooled by the Peltier effect. The spectral range varied, but in all cases was extended down to 100 cm^{-1}. Spectra were recorded without any preparation of the samples, the latter simply being laid on a metal support. After focusing on a crystal through a microscope and a CCD camera, the spectrum was recorded with a variable number of scans or an accumulation time according to the intrinsic signal intensity.

The infrared and Raman spectra of many commercial pigments/minerals were also recorded for comparison purposes.

FT–IR spectroscopy

This technique was, with the aid of a PerkinElmer Model 1700 spectrophotometer, used to search for traces of organic medium in the inorganic powders drawn from plasters. For this purpose, 1 mg of the sample was uniformly ground in an agate mortar together with 100 mg of dried KBr; this powder was then pressed inside a cylindrical mould using a load of about 10 MPa to obtain a 13 mm diameter pellet.

X-ray diffraction

This analytical technique identifies the crystalline components of samples. Analysis was carried out on the various layers of plaster, on the pigmented powder and, where the sample size allowed, on the surface of the fragment inserted in the diffraction chamber.

A Panalytical Model X-pert pro XRD machine was used, with CuKα incident radiation and an Ni filter, at 40 mA and 40 kV. Scanning was continuous between 5° [2θ] and 52° [2θ].

Colorimetry

Colorimetric analysis was achieved using an UV-VIS spectrophotometer in reflectance mode. It was possible to obtain **L**, **a** and **b** values—on the HUNTERLAB system—throughout the reflectance curve.

The instrument was a PerkinElmer Lambda Bio 20, equipped with a 10 cm diameter integration sphere, operating in the range from 380 nm to 780 nm, with a scan rate of 480 nm min^{-1} and a D65 illuminator.

EXPERIMENTAL DATA AND RESULTS

Cross-section images from the optical microscope

The stratigraphy of some of the plasters is illustrated in Figures 2 (a) and 3 (a). Figure 2 (a), for instance, clearly shows all the layers of the plaster, including the pigmented one.

The stratigraphy of sample 1 shows a layer of plaster with dark clasts and a layer of red pigment clearly separated from the substrate. Sample 1 has three layers: the white plaster, the red-pigmented zone and a thin black surface layer. One of the aims of further analysis was thus to clarify whether this black layer was caused by chemical degradation or applied deliberately.

This was the case with a number of samples: the surface of plaster 2, for instance, has a red pigment with traces of a black one, an association that may be an inherent part of the craftsmanship or the result of chemical degradation of the red pigment itself.

The surface of sample 5 is characterized by a brilliant green pigment. The thus-pigmented surface of the plaster is highly polished and this can be ascribed to a lime layer formed by carbonation.

Initial optical analysis suggests that the regular black clusters inside the plaster layers can be assigned to quartz or calcite.

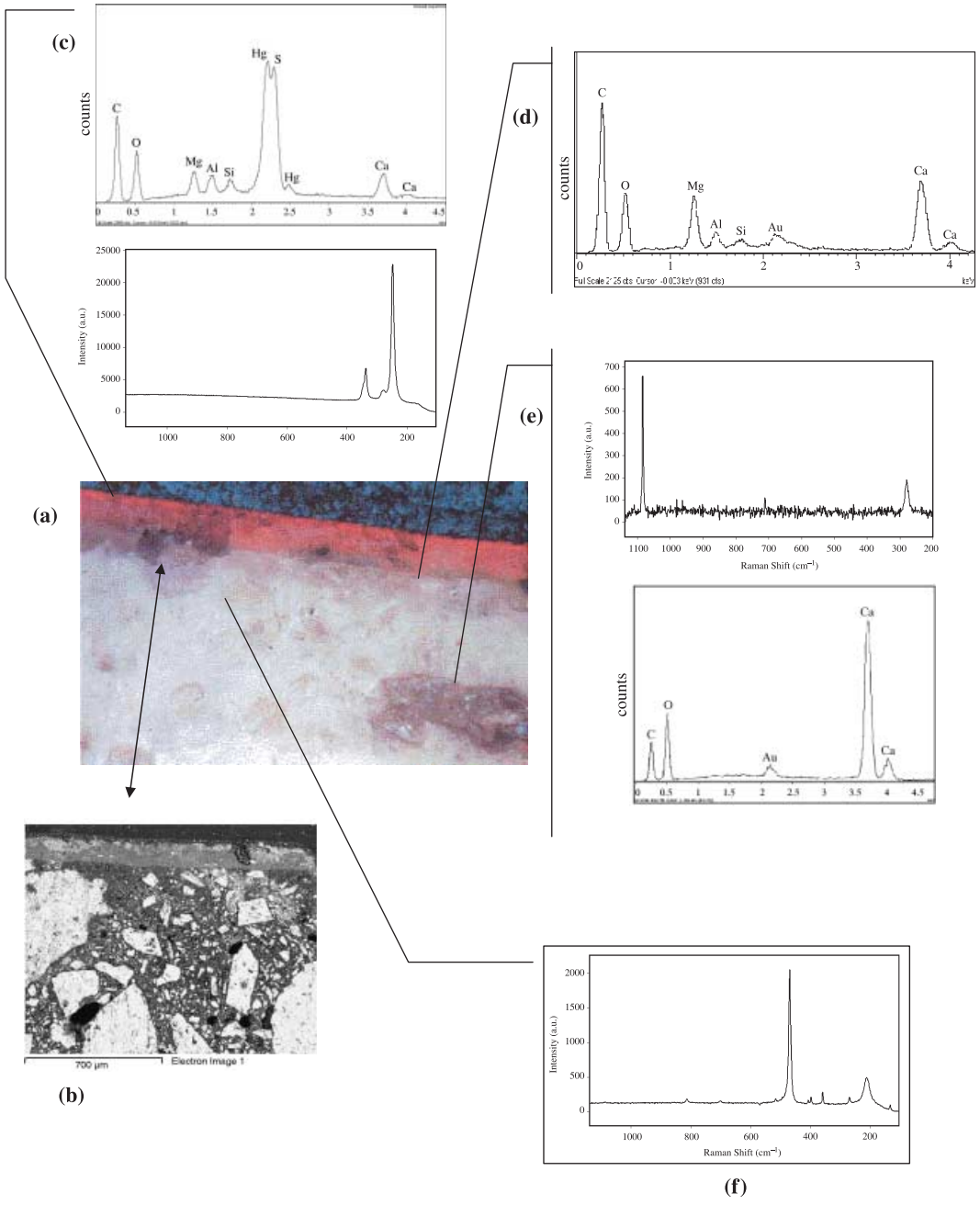

Figure 2 (*a) A cross-section of plaster 1.* (*b) An SEM image of the section.* (*c) EDS* (*top) and micro-Raman analysis* (*bottom) of a granule of the red surface.* (*d) EDS analysis of the superficial cream pigment.* (*e) EDS* (*top) and micro-Raman analysis* (*bottom*) (*1150–120 cm*$^{-1}$) *of a dark-coloured crystal.* (*f) The micro-Raman spectrum* (*1100–120 cm*$^{-1}$) *of a white crystal.*

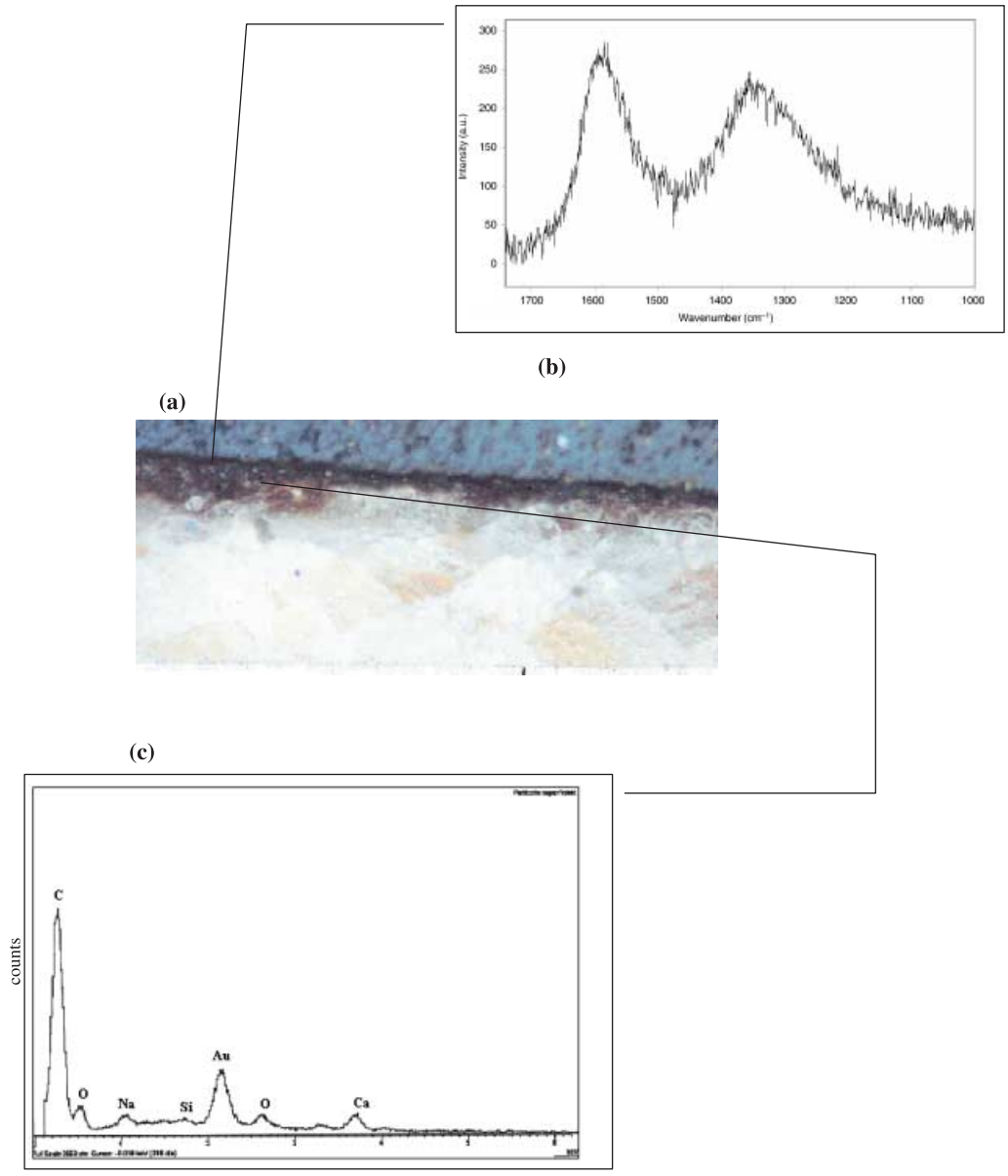

Figure 3 (*a) A cross-section of plaster 34*. (*b) A micro-Raman spectrum* (*1850–900 cm*$^{-1}$) *collected on the black surface*. (*c) EDS analysis of the superficial dark pigment*.

SEM–EDS

All prepared cross-sections were analysed via the scanning electron microscope: relevant results are shown in Table 1.

Figure 2 (a) illustrates the plaster cross-section: the bigger, brightly coloured crystals were identified, on the basis of Ca, C and O EDS signals, as calcite ($CaCO_3$) (Fig. 2 (e)).

Table 1 *Pigments found in the plaster surfaces by micro-Raman and by FT–IR spectroscopy (C = carbon, Ca = calcite, Ci = cinnabar, EB = Egyptian Blue, GE = Green Earth, Go = goethite, He = hematite, Mg = magnetite, Ww = whitewash)*

		Minerals or pigments	
Plaster	*Colours*	*Raman*	*FT–IR*
1	White, black, red	Ci, C	Ca, dolomite, Ci, GE, Ww
2	Green, white, red	C, Go, black Ci	Red ochre, GE, Ww
3	Green, red	C, Go, Ci	GE
4	White, grey	C, Go, C	Ww, lampblack
5	Green, red	C, He, Mg, Ci	Ci, GE
6	Cream	He, Go	Go, Ww
7	Green	C, He	GE
8	Green	C, He	FeS_2, GE
10	Creamy	C, He, Mg	Go, Ww
11	Green, cream, black	C, Go, C, GE, Eb	Go, GE, Ww, lampblack
12	Red, black	He, Mg	Lampblack, red ochre
13	Red	C, He	Red ochre
14	Red	He, Mg	Ci
15	Red	Go	Silica, He, Go, Ci
16	Cream, red	C, Go, Ci	Go, red ochre
17	White	C	Ww
18	Two different reds	C, He	Red ochre, Ci
19	Two different reds	C, He, Mg	Red ochre, Ci
20	Red	C, He	Ci
21	Cream	C, Go	Go, Ww
22	Cream, black	C, Go, He	Go, Ww, lampblack
23	White	C	Ww
24	White, black	C	Ww, lampblack
25	Black	C, He	Lampblack
26	Black	C	Lampblack
27	White	C	Ww
28	White	C	Ww
29	White	C	Ww
30	White	C	Ww
31	Cream	C, Go	Go, Ww
32	Red	C, He	Red ochre
33	Red	C, He	Ci
34	Black	C	Lampblack
35	Black	C	Lampblack
36	Black	C	Lampblack
37	Red	C, He	$BaSO_4$, red ochre, Ci

Microstructural and elemental analyses of plasters revealed the expected results: on the pigmented layer (Fig. 2 (d)), Ca, Mg, C and O were found. Dolomite ($CaMg(CO_3)_2$), as opposed to huntite ($CaMg_3(CO_3)_4$), is present in the matrix: the former is a crystalline component frequently found in the pigmented layer, while the latter is only identified more rarely (Farmer 1974; Fagnano *et al*. 2003; Ambers 2004).

The EDS spectrum from the green surface of plaster 5 does not identify the specific atoms needed for recognition of a particular pigment; however, the simultaneous presence of Si, Al,

K and Fe hints at the probable use of a pigment such as 'Natural *Terrae*' or 'Green Earths'. These pigments might be aluminosilicates of Fe and K (like chlorite or similar) or celadonite and glauconite. As usual, the plaster layer consists of lime and sand.

Several other analyses provided similar results. The presence of Mg, K and Na signals reveals the presence of '*arriccio*', the base plaster consisting of calcite and silica, and the clay components. No significant proportions of these compounds are found in the '*intonachino*', the finer particle size plaster used for pigment applications just below the pigmented surface. Of course, calcium carbonate and silica compounds are present in higher concentrations in all the samples.

Microanalysis of the yellowish surface of plaster 6 reveals iron and oxygen, thereby indicating the presence of iron oxides. The same results are obtained in plaster 11, in which colorimetric analyses (see the 'Colorimetric analysis' section) give similar chromatic behaviour. The luminance **L** of this pigment is higher. Is not clear which iron oxide it is, but—very often, for this kind of yellow—goethite [α-FeO(OH)] is employed, or a mixture of oxides is present (as a part of a yellow ochre). Micro-analysis of red surfaces shows that the Romans obtained this colour using different pigments based on iron and mercury compounds. Analysis of the white particles (mean dimension > 100 μm) in plaster 15 identified a composition based on SiO_2; it can therefore be supposed that bigger sand grains were used in these layers.

EDS analysis of cross-sections of samples with black surfaces, such as plaster 34 (Fig. 3 (a)), gave a very high carbon signal (Fig. 3 (c)), a result confirmed by the micro-Raman spectrum (Fig. 3 (b)); the charring of vegetal materials was, in effect, a widespread lampblack preparation practice in antiquity. Further EDS analysis of this same sample (number 34) also showed that the white surface was obtained by using whitewash. Moreover, EDS analyses also recorded C, O, Ca and Mg signals, thus suggesting the presence of some dolomite. Cinnabar (HgS) was used to obtain bright red surfaces, whereas iron oxides were used for dark red surfaces. Elemental pigment layer analysis of plaster 37, when compared with that of plaster 1, highlights the presence of Ca, C and O (calcite) only. In this layer, cinnabar is mixed in with calcite in lower concentrations than in plaster 1.

Identifying iron oxides as pigments through SEM–EDS was far from simple: with Raman microscopy, it was somewhat easier. In fact, the EDS results for iron-containing red pigments are not so different from those for the surfaces of yellow ochre.

In plaster 8, some spherical crystals were found (10 μm in diameter) (Fig. 4 (b)) and punctual analysis revealed only Fe and S: it is therefore reasonable to assume the presence of pyrite, FeS_2 (Fig. 4 (a)). While this mineral is very common in nature, this particular shape is unusual, and it is probably due to mechanical treatment by the craftsman at work or the result of a particular deposition.

Micro-Raman spectroscopy

Table 1 shows all the surface constituents identified by effecting micro-Raman analysis directly on the fragments.

Figure 2 (e) shows a Raman spectrum obtained by focusing the laser on a dark crystal within plaster 1. Three bands are present in this spectrum: a strong one at 1084 cm^{-1} and two weaker ones at 713 and 280 cm^{-1}, the bands typical of calcite. This compound was identified in all the plasters and also on the surface of a few cross-sections: this is consistent with the fresco mural painting technique of the Roman age.

Figure 2 (f) shows the spectrum of a central zone of the plaster, where the characteristic strong band of SiO_2 as crystalline quartz at 467 cm^{-1} is present; this can be imputed to the

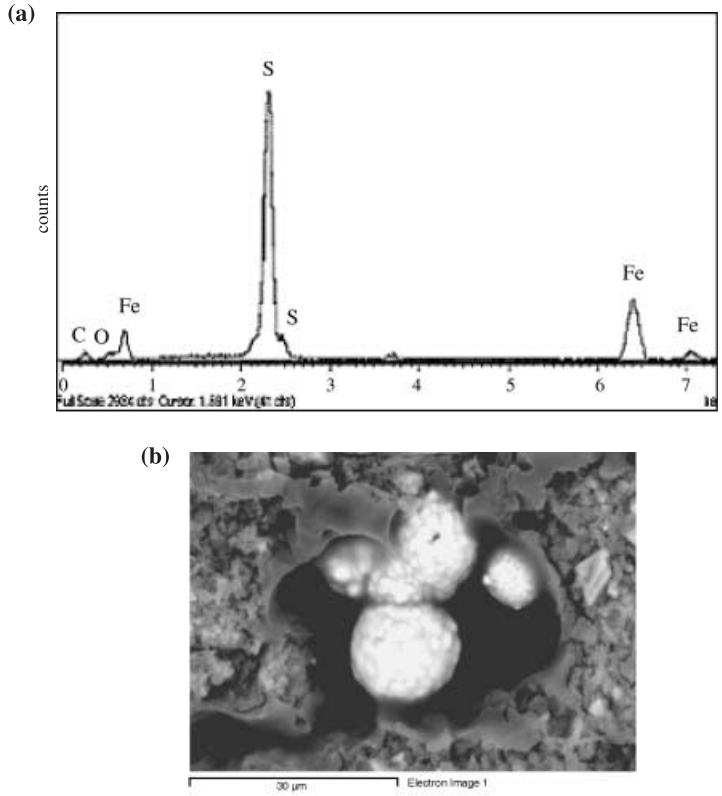

Figure 4 *EDS analysis of the white surface of plaster 8 and an SEM image (1780×) of the spherical shape of pyrite.*

symmetric stretching of O–Si–O groups. The Raman spectrum of the red-pigmented surface in plaster 5 indicates a very strong band at 254 cm^{-1} and a weaker one at 350 cm^{-1}. These are the 'fingerprints' of red cinnabar (α-HgS).

A different red pigment was found in plaster 15. The layer is thicker than for cinnabar and without any clear separation from the plaster layer; the colour is also different, being closer to brick red than vermilion red. A micro-Raman spectrum (Fig. 5) of this layer identifies this pigment as hematite, the crystalline form of the Fe_2O_3 oxide. The characteristic bands of this pigment are the strong ones at 218 and 280 cm^{-1} and the weaker ones at 405, 498 and 610 cm^{-1} (Bersani *et al*. 1999). By using Raman spectroscopy for the analysis of red surface samples we were, at least, able to identify cinnabar and hematite.

Plaster 11 has a yellow ochre surface, and a rather different, more complex, stratigraphy than the others. The pigmented layer bears a dark patina and the plaster has a heterogeneous structure. The strong band at 390 cm^{-1}, joined to those at 547 and 477 cm^{-1}, together with the ones at 294, 240 and 202 cm^{-1}, can be attributed to the presence of goethite (γ-FeOOH). This mineral is often mixed in with other iron oxides (such as hematite and magnetite), to constitute what are called yellow ochres. However, in this sample, Raman spectroscopy identified only traces of hematite. Other forms of analysis (SEM–EDS and FT–IR spectroscopy) of these yellow surfaces confirmed that the constituents of the pigmented layers are, in effect, FeOOH and Fe_2O_3.

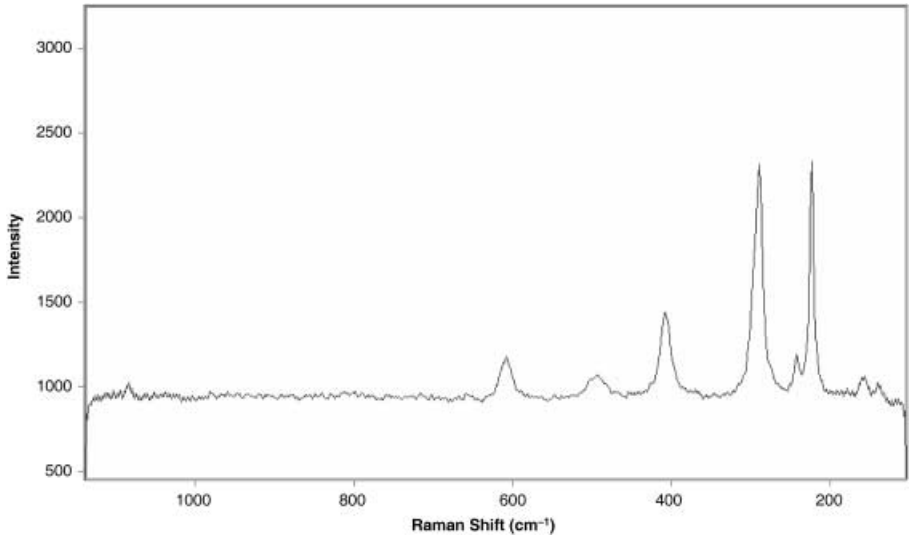

Figure 5 *The micro-Raman spectrum of a red area of plaster 15.*

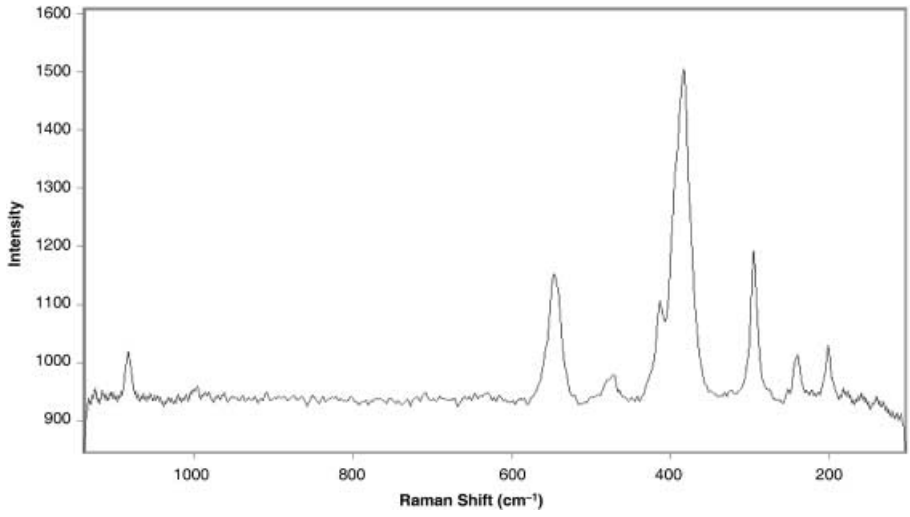

Figure 6 *The micro-Raman spectrum collected on a yellow crystal of the surface of plaster 21.*

Raman spectroscopy of the yellow surface of plaster 21 (Fig. 6) indicates the presence of three different components: from bands at 387 and 480 cm^{-1}, goethite (FeOOH), as seen in plaster 11, the characteristic hematite bands and, at higher wavenumbers, the calcite bands.

The surface of plaster 11 also has green areas (Fig. 7): here, broad bands at 268, 317, 385, 455, 546 and 698 cm^{-1} come close to the wavenumbers of celadonite (light blue) and glauconite (green); these are the main components of *Terra Verde* (*Appianum*, or Green Earth), which was used extensively by the Romans in wall paintings. Incidentally, on Monte Baldo, near Verona (about 100 km from *Mutina*), there are still *Terra Verde* mines.

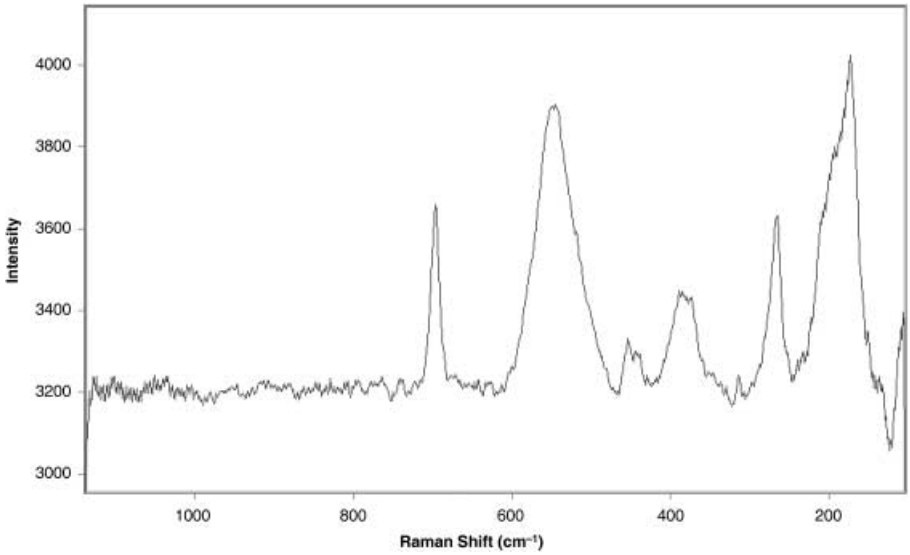

Figure 7 *The micro-Raman spectrum (1100–100 cm^{-1}) collected on the green surface of plaster 11.*

In the green layers of plaster 11, dark blue crystals mixed with Green Earth (dimensions 10–30 μm) can be seen. These crystals show a very weak Raman effect with the 632 nm laser, but a main band at 432 cm^{-1} is sufficient to reveal the presence of Egyptian Blue (Barbet *et al.* 1997; Vinella 2000; Baraldi 2001; Ambers 2004; Baraldi *et al.* 2005). The infrared spectrum confirms this. This is the only green sample with this particular composition. The spectra for green plasters 7 and 11 coincide with the others, highlighting the presence of goethite and iron oxides.

Analysis of black pigments was easily carried out via micro-Raman spectroscopy. The pigmented layers were generally shown to consist of calcite and amorphous carbon, which sometimes appeared together in the spectrum, both when the analysis was done on the surface of the cross-section and in the sample surface itself. In fact, the micro-Raman spectrum (Fig. 3 (d)) showed the presence of carbon (two slightly overlapping broad bands at 1340 and 1580 cm^{-1}) and a weak peak at 1084 cm^{-1} (calcite). The characteristic bands of amorphous carbon reported in the literature are band D (1350 cm^{-1}) and band G (1660 cm^{-1}). The former is due to the vibration of disordered carbon of the ν_{C-C} kind and the latter to $\nu_{C=C}$ vibrations.

On the same sample, cream-coloured surfaces have a spectrum indicating the presence of calcite, and sometimes quartz, without any chromophore.

FT–IR spectroscopy

Some representative samples were chosen for Fourier transform infrared spectroscopy analysis. FT–IR transmittance was recorded from 4000 to 400 cm^{-1}. All spectra reveal the presence of calcite and silica and confirm the complete absence of organic media (Farmer 1974; Bèarat *et al.* 1997; Fagnano *et al.* 2003).

Figure 8 shows a typical fine-plaster IR spectrum in which the characteristic peaks of calcite are easily recognized. The weak band at 1410 cm^{-1} is due to asymmetric stretching (active in

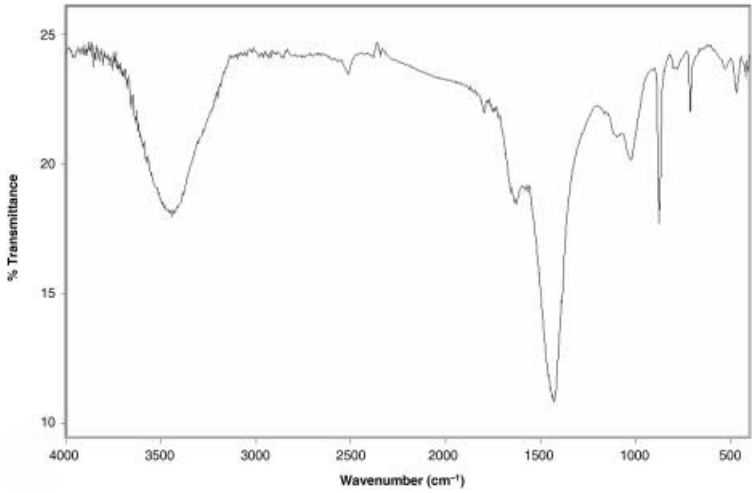

Figure 8 *An FT–IR spectrum of a typical fine plaster.*

IR but inactive in Raman) of the CO_3^{2-} group, and the sharp one, at 880 cm^{-1}, is due to its asymmetric bending. The other calcite-related signals are the band at 708 cm^{-1} (in-plane bending of the carbonate ion, corresponding to the observed Raman band at 713 cm^{-1}) and the weak peaks at 1798 and 2511 cm^{-1}, which are combination and overtone bands.

In the IR spectrum, the presence of peaks at 1096 and 1020 cm^{-1} suggests the presence of silica; they correspond precisely to the asymmetric stretching vibrations. Some peaks at 1621, 1145, 1121, 680 and 601 cm^{-1} reveal the presence of gypsum ($CaSO_4 \cdot 2H_2O$). Recognition of dolomite in the presence of a large proportion of calcite is difficult in IR spectra, because its characteristic peak is at 1473 cm^{-1} and is thus overlapped by the stronger calcite signal at 1430 cm^{-1}. However, the deformation band at 725 cm^{-1} can be distinguished from the corresponding calcite band at 713 cm^{-1}.

Of course, FT–IR spectra for the base plaster, '*arriccio*' and '*intonachino*' are very similar, and are all overwhelmed by the calcite spectrum.

This analytical technique failed to reveal the presence of any organic medium on the surfaces of the cross-sections: although the medium concentration would be expected to be low, it would still have been observable in the spectrum, through the stretching bands of the CH_3 and CH_2 groups in the 2800–3000 cm^{-1} region (Bèarat *et al.* 1997; Vinella 2000).

All the obtained data are summarized in Table 1.

Diffractometric analysis

Some XRD diffractograms were studied and compared with spectroscopic data. These analyses were carried out on plaster powders, pigmented layer powders and also directly on some of the sample surfaces. Crystalline phases were identified using a PDF database (Mineral Powder Diffraction File, International Centre for Diffraction Data): this lists all the **d** values together with the relative intensities of the peaks and other specific parameters for each crystalline phase.

Calcite and quartz are the predominant phases highlighted by XRPD analysis. A high number of samples feature calcareous matrices with similar behaviour patterns. In the analysis

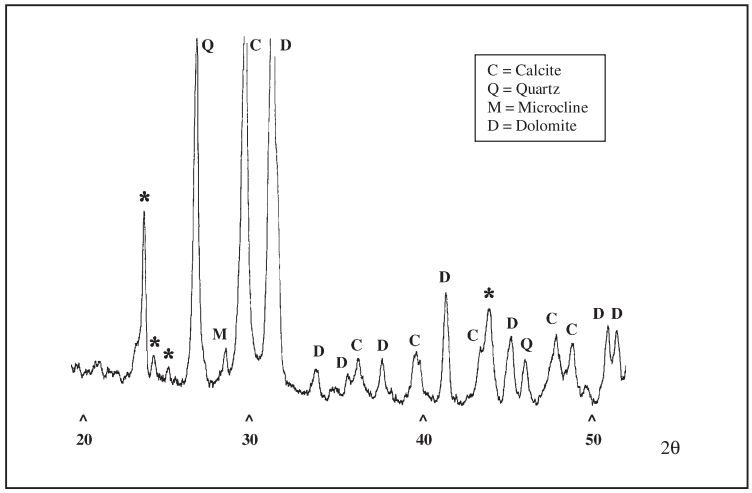

Figure 9 *XRPD on the red surface of plaster 3.*

of the '*arriccio*', the following compounds were frequently detected: albite ($NaAlSi_3O_8$), microcline ($KAlSi_3O_8$) and the characteristic calcareous matrix (calcite and quartz).

Figure 9 is the XRPD spectrum of plaster 3: the very strong peak is dolomite related. This crystalline phase is observed in some samples; for example, plaster 7. In this case it was possible to assess an enrichment of dolomite in the surface layer. Assignation of the signals marked with asterisks—the peaks with the **d** spacing values at 3.79 (23.4 2θ), 3.70 (24.0 2θ), 3.58 (24.9 2θ) and 2.07 (43.7 2θ)—was difficult. The strongest peak is probably related to the presence of gypsum, but the other characteristic signals of this compound are absent. Peaks at 23.4 2θ and 43.7 2θ may be related to calcium silicate (very improbable) or to lazurite ($Na_6Ca_2Al_6Si_6O_{24}SO_4$), but this is a blue pigment, whereas the surface is red. Moreover, there is no record of lazurite being used as a pigment in the Roman age.

XRPD analysis of the green-pigmented surface of plaster 7 was also carried out. It shows the presence of some crystalline phases and, among these, a micaceous mineral, like muscovite ($KAl_2Si_3AlO_{10}(OH)_2$), and a chloritic clay, both present in low proportions within illite. In muscovite and chlorite ($Mg_3(Mg_2Al)(Si_3Al)O_{10}(OH)_8$), the cation Fe^{2+} might substitute the Mg^{2+} and thereby the colour turns greenish. These are also identified via SEM–EDS, as was the hematite. Peaks 34.9 2θ and 37.6 2θ remain unidentified.

Thermal analysis (TG/DTA)

Simultaneous thermal analysis was carried out on selected, differently pigmented micro-samples taken from the plasters (from 3 to 15 mg). Thermograms for the red-coloured surface of plaster 26 and its '*arriccio*' are shown in Figure 10 for comparison purposes. The only appreciable thermal effect is the one illustrating thermal decomposition of $CaCO_3$ to calcium oxide and carbon dioxide, as ascertained by the endothermal peak at about 765°C.

For the '*arriccio*', the endothermal peak at 569°C is consistent with the transformation of α quartz $\rightarrow$ β quartz, present in significant proportions in this layer.

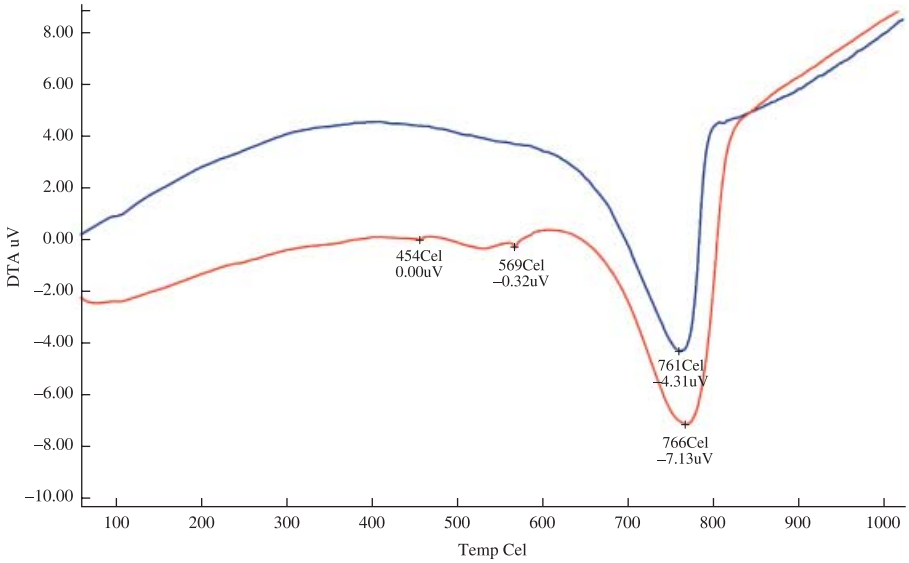

Figure 10 *A comparison of the DTA analysis of the* 'arriccio' *(red line) and fine plaster (blue line) of plaster 26.*

Moreover, in the '*arriccio*', a weak endothermal effect at 454°C, unrelated to a weight loss in TG, had to be assigned to another transition or transformation of unknown origin. Unfortunately, none of the pigmented layer thermal traces can be ascribed to chromophoric materials, even though iron oxides or hydroxides, used as red pigments, should have endothermal effects at 280°C or 340°C (e.g., goethite).

Two different red-pigmented surfaces were analysed: plasters 13 and 26. However, in these thermograms only the thermal decomposition of calcite can be observed. The low sensitivity of the TG/DTA technique is again evident here, as it is unable to reveal decomposition effects for low concentrations of pigments in a calcareous matrix.

Colorimetric analysis

Colorimetric analysis of the plaster surfaces was carried out by using a reflectance spectrophotometer and evaluating CIELAB parameters. A summary of the obtained values is given in Table 2.

Graphic representation of **L**, **a** and **b** values enables colour comparison in terms of the brilliance and tone of the pigmented surfaces. Evaluation of—and the ratio between—these parameters can, in the light of the microstructural, spectroscopic and diffractometric analyses of sample surfaces, help to characterize the used pigments.

Figure 11 (a) shows the CIELAB representation of a comparison between different red samples. For instance, plaster 26 has a very high **b** value (tending towards yellow) compared to the other red plaster, number 18, and a very low **L** value (much darker). The chromatic differences between surfaces of similar shades can be ascribed to different pigments (cinnabar or iron oxide, in this example) or different concentrations of the pigment in the medium.

A comparison between yellow-pigmented samples is shown in Figure 11 (b), which provides data on plasters 11, 16, 21 and 22. They appear to belong to the same wall, having the same

Table 2 *The **L**, **a** and **b** parameters of the plaster's CIELAB colorimetric analysis*

Plaster	***L***	***A***	***b***
1 white	81.85	6.05	14.22
27 white	78.76	2.95	8.21
28 white	80.65	2.33	5.18
29 white	86.04	5.40	9.58
30 white	83.06	4.23	9.30
2 green	89.34	–0.18	2.50
3 green	89.99	0.68	2.11
5 green	89.78	–1.07	0.99
7 green	89.05	–0.68	3.52
8 green	91.17	1.08	5.11
11 green	94.92	0.19	–1.62
10 yellow	70.14	18.34	38.35
11 yellow	69.25	15.35	28.13
16 yellow	66.23	18.93	30.27
21 yellow	66.32	13.70	28.73
22 yellow	66.39	13.38	24.29
1 red	55.64	23.52	20.87
2 red	57.70	17.87	15.09
3 red	57.49	23.72	17.33
5 red	54.52	21.65	11.55
13 red	57.70	17.87	15.09
18 red	54.55	13.71	2.08
19 red	64.71	21.91	14.62
20 red	52.03	15.44	2.51
25 red	55.82	9.03	6.02
26 red	41.64	7.47	35.05
33 red	57.70	17.87	15.09

yellow ochre colour on the surface and a very similar brilliance, even though the **a** and **b** values differ slightly. The pigment used to obtain the colour on the sample surface is goethite.

Figure 11 (c) shows the CIELAB representation of analysis carried out on the green surfaces of plasters 2, 3, 5, 7, 8 and 11.

The **b** value (negative to blue) for plaster 11 differs in brilliance from that of the other plasters (but this value could be an outlier).

Green surfaces have very homogeneous **a** values, between −1.07 and 1.08, with **b** values varying more from −1.62 to 5.11. In any case, the green tones are very similar, even though different pigments are employed (Green Earth and Egyptian Blue).

Colour analyses of five plasters (plasters 1, 27, 28, 29 and 30) with white surfaces proved ineffective (Fig. 11), as the difference between CIELAB parameters is very high, probably due to alteration of the surfaces.

DISCUSSION AND CONCLUSIONS

The aim of this work was to try to characterize the Roman plaster-making and 'fresco' painting techniques employed in *Mutina*, using several analytical tools. Results were compared in

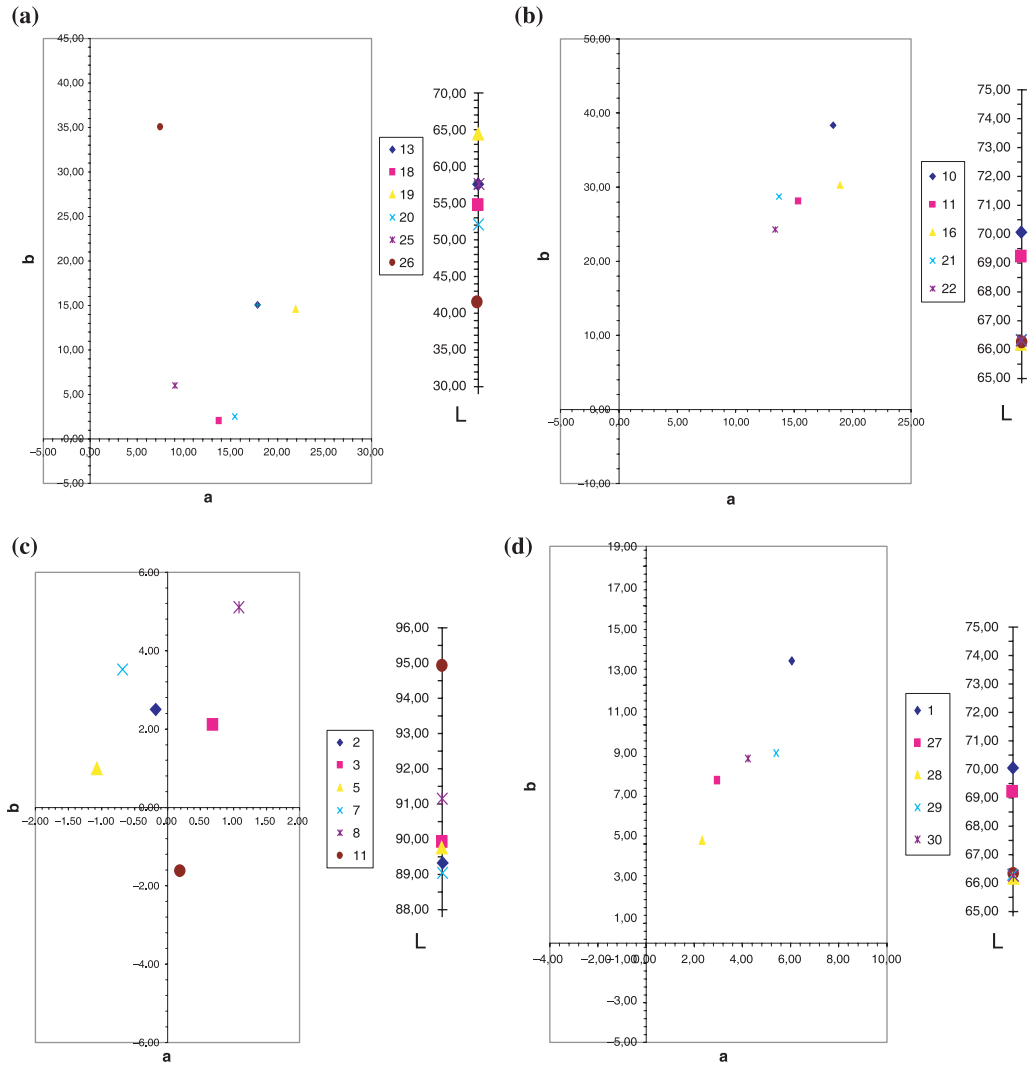

Figure 11 (*a*) *A CIELAB representation of the colorimetric analysis of the red pigments of plasters 13, 18, 19, 20, 25 and 26.* (*b*) *A CIELAB representation of the colorimetric analysis of the yellow pigments of plasters 10, 11, 16, 21 and 22.* (*c*) *A CIELAB representation of the colorimetric analysis of the green pigments of plasters 2, 3, 5, 7, 8 and 11.* (*d*) *A CIELAB representation of the colorimetric analysis of the creamy white pigments of plasters 1, 27, 28, 29 and 30.*

order to check the reliability of these different analytical techniques. The results thus obtained can be compared with the literature concerning Roman wall paintings in northern Italy, an aspect that is highly useful for both analytical and structural investigation, and for the artistic and archaeological analysis of the samples (Barbet *et al.* 1997; Bèarat *et al.* 1997; Colinart and Menu 2001; Barbet 2002; Baraldi *et al.* 2005). Comparisons made together with the authors of research in adjacent areas has revealed a similar, but not identical, palette. For example, *Aemilia* lepidocrocite is sometimes detected in the region instead of goethite,

thereby indicating the use of locally found yellow ochres rich in that mineral. On the basis of present comparisons, the same pigment-mixing rules are observed (e.g., a mixture of Egyptian Blue and Green Earth to get emerald green). Moreover, the use of aragonite as opposed to calcite is observed for the painting of white lines on coloured surfaces (Mazzocchin *et al.* 2004).

Plaster layers

Composition is very simple, being based, of course, on an air–ligand medium: the components of the '*arriccio*' are lime and sand, as are those of the surface layer. SEM–EDS microstructural analysis and observation of cross-section stratigraphy with an optical microscope confirm the use of raw calcareous plaster and large grains (100 μm) of silica sand.

Elemental analysis and XRPD reveal, for some samples (plasters 1, 2, 3, 8, 11, 13 and 15), an enrichment of the '*arriccio*' with clay minerals (potassium and sodium aluminosilicates), probably so as to modify the rheological properties of the paste (to 'fatten up the plaster') and thus improve cohesion. This presence of clay minerals may, however, be accidental because of the natural abundance of such minerals in calcareous rocks.

Dolomite is frequently detected, especially in the surface layers: it may, therefore, have been added intentionally to lower the particle size distribution and so enhance the quality of the painting and opacify the plaster. However, SEM–EDS Mg, K and Na signals and XRPD peaks for dolomite and aluminosilicates are very weak in comparison with those of lime and sand.

These Roman plasters have a silica–calcareous structure, with high porosity and non-cohesive grains.

XRD analysis of the painted surfaces of samples 1 and 7 shows the presence of muscovite, chlorite and weak illite-related peaking, as confirmed by SEM–EDS analysis. None of the previously found phases were detected by thermal analyses, a fact probably explained by their low endothermal response (as opposed to the significant endothermal response of the carbonate matrix).

Separation between the '*arriccio*' and pigmented layers was always very sharp and could be observed via either the scanning electron microscope or the optical microscope. SEM–EDS analysis of these calcareous matrices also highlighted the occasional presence of other components, such as spherical pyrite (FeS_2) crystals.

Pigments

Through comparison of different analytical results, an attempt was made to identify the pigments used by the Romans in *Mutina* in the second century AD. The presence of organic dyes such as indigo (blue or greenish blue) or saffron (yellow) has been excluded (although they are sometimes recognized in Roman plasters).

Creamy plasters Creamy surfaces were obtained by using whitewash. The analytical data excludes the presence of lead (and therefore white lead) or any enrichment of the binder–pigment suspension with gypsum or fossil flour.

In creamy plasters (6, 10, 16, 21 and 31), pigments such as goethite and whitewash were identified. It is a known fact (Barbet 2002) that to obtain different shades of yellow, different proportions of iron oxide were added to goethite, or yellow ochre was heated to different

temperatures. In fact, the surface micro-Raman spectra for yellow plasters 6, 10 and 11 show the specific goethite bands and also some hematite and magnetite peaks.

White plasters As mentioned above, white surfaces were obtained by using whitewash. Once again, the presence of lead, or the enrichment of the binder–pigment suspension with gypsum or fossil flour, were excluded.

White plasters are seen in samples 17, 24, 28, 27, 29 and 30. Analysis reveals the presence of only whitewash in their pigmented layer.

Red plasters As mentioned in the 'Thermal analysis' section, red-pigmented surfaces exhibit a variety of brilliance and tone.

Plasters 1, 2, 3 and 5 have bright red, well-preserved surfaces. No surface pigments were found and the characteristic colour of the surface can only be attributed to pigments mixed into the plaster surface layer, and perhaps also to the technique used to apply them.

EDS analysis of plasters 1 and 5 (cross-sections) and punctual analysis by micro-Raman spectroscopy confirm the presence of cinnabar or vermilion. Red dyes have been excluded, since there was no high-fluorescence background in any of the samples.

EDS analysis of other red surface samples (e.g., plasters 2, 18 and 37) highlights the presence of iron and oxygen together with calcareous matrix. This is due to the presence of hematite, as confirmed by Raman spectroscopy, which sometimes identifies it where mixed with goethite, when the colour tends towards yellow.

The other red plasters are numbers 13, 14, 15, 19, 20, 32 and 33 (see Table 1). Plasters 18 and 19 contain both kinds of red pigment (cinnabar and red ochre).

Green plasters Green surface plasters (numbers 1, 2, 3, 5, 7, 8 and 11) probably used Green Earth and Egyptian Blue, mixed together.

Microanalysis and XRD analysis of green plasters 5 and 7 also show the presence of aluminium silicates such as chlorite and muscovite.

Plasters 7 and 8 and plasters 5 and 11 would appear to belong—as suggested by surface analysis and cross-section observation—to different wall paintings of the *Domus*. Malachite ($Cu_2CO_3(OH)_2$) was never found.

These green-pigmented surfaces show varying degrees of alteration, probably because of different levels of chemical aggression (e.g., moisture or soluble salt variations inside the wall).

Black plasters Black surfaces were obtained using amorphous carbon-black, as easily ascertained by the micro-Raman spectra with bands at 1360 and 1590 cm^{-1}. The black plaster samples are numbers 25, 26, 34, 35 and 36.

The use of Raman spectra also made it possible to identify the black cinnabar: the formula and crystalline structure are the same as in its more common red counterpart, the transformation into black probably being due to contact with humidity.

The pigment palette used by *Mutina* craftsmen is very simple compared to the Pompeian one (Fagnano *et al*. 2003; Ambers 2004).

The medium used in the layers

Any use of organic binders in the layers could be excluded: the FT–IR and micro-Raman spectra do not exhibit any of the bands assignable to organic compounds.

As is evident in the cross-sections and SEM images, the plaster pigments of the *Domus* are always contained in a calcareous matrix. It can thus be said that the 'fresco' technique was used on these walls. This technique uses lime as the medium: calcium hydroxide is mixed with pigments in water and layered on the wall.

REFERENCES

Ambers, J., 2004, Raman analysis of pigments from the Egyptian Old Kingdom, *Journal of Raman Spectroscopy*, **35**, 768–73.

Augusti, S., 1967, *I colori pompeiani*, De Luca Ed., Rome.

Baraldi, P., 2001, Study of the vibrational spectrum of cuprorivaite, *Annali di Chimica*, **91**, 679–90.

Baraldi, P., Catarsi dall'Aglio, M., Bersani, D., and Lottici, P. P., 2005, Micro-Raman and FTIR analysis of Roman painted plasters coming from archaeological sites in Parma (Italy), Paper presented at the III Congress 'Raman in Art and Archaeology', Paris, 2005.

Barbet, A., 2002, *La pittura romana: dal pictor al restaurator*, University Press, Bologna-Imola.

Barbet, A., Coupry, C., and Lautie, A., 1997, Apport de la spectrométrie Raman à la caractérisation de peintures murales, in *Roman wall painting: materials, techniques, analysis and conservation* (eds. H. Bèarat, M. Fuchs, M. Maggetti and D. Paunier), 257–68, Institute of Mineralogy and Petrology, Fribourg University; see especially p. 261.

Bèarat, H., Fuchs, M., Maggetti, M., and Paunier, D. (eds.), 1997, *Roman wall painting: materials, techniques, analysis and conservation*, chs I–III, Institute of Mineralogy and Petrology, Fribourg University.

Bersani, D., Lottici, P. P., and Montenero, A., 1999, Micro-Raman investigation of iron oxide films and powders produced by sol–gel synthesis, *Journal of Raman Spectroscopy*, **30**, 355–60.

Casoli, S., 1999, *Painted plasters of the Domus in Farini Street in Modena*, Ph.D. thesis, University of Bologna.

Ciliberto, E., and Spoto, G. (eds.), 2000, *Modern analytical methods in art and archaeology*, Chemical Analysis Series, vol. 155, Wiley-Interscience, New York.

Colinart, S., and Menu, M. (eds.), 2001, *La matière picturale: fresque et peinture murale*, Edipuglia, Bari.

Fagnano, C., Tinti, A., Taddei, P., and Baraldi, P., 2003, La tavolozza dei colori negli affreschi di Pompei, in *Ricordo di Alessandro Bertoluzza*, 125–37, Clueb, Bologna.

Farmer, V. C., 1974, *The infrared spectra of minerals*, Mineralogical Society, London.

Mazzocchin, G. A., Agnoli, F., and Salvadori, M., 2004, Analysis of Roman age wall paintings, *Talanta*, **64**, 732–41.

Vinella, M., 2000, *Studio di tecniche avanzate di acquisizione di spettri vibrazionali su matrici solide*, Doctoral thesis, University of Modena.

Vitruvius, P., 1960, *De architectura*, S. Ferri Ed., Roma.